

# Hysteresis in an Ising model with mobile bonds

D. Čapeta and D.K. Sunko

*Department of Physics,  
Faculty of Science,  
University of Zagreb,  
Bijenička cesta 32,  
HR-10000 Zagreb, Croatia.*

Hysteresis is studied in a disordered Ising model in which diffusion of antiferromagnetic bonds is allowed in addition to spin flips. Saturation behavior changes to a figure-eight loop when diffusion is introduced. The upper and lower fields delimiting the figure-eight are determined by the Hamiltonian, while its surface and the crossing point depend on the temperature and details of the dynamics. The main avalanche is associated with the disappearance of hidden order. Some experimental observations of figure-eight anomalies are discussed. It is argued they are a signal of a transient rearrangement of domain couplings, characteristic of amorphous and/or magnetically soft samples, and similar to evolution of kinetic glasses.

## I. INTRODUCTION

Magnetic hysteresis is a classic example of metastability at experimentally easily accessible time scales. Its ready appearance under simple conditions makes it not only technologically important, but also a theoretical challenge. In addition to macroscopic approaches, relying on multiply-valued equations of state, there has been considerable work done over the past decade in Monte Carlo simulations of lattice systems. The high reproducibility of hysteresis curves, and the fact that among their many observed shapes most are fairly simple, imply that hysteretic delay involves processes similar to ordinary thermalization, which can be modeled by a simple random walk. It is thus reasonable to ask, which features need to be added to the walker in order to reproduce some particular aspect of the experimental observations.

The Ising model, in the widest sense, has evolved as an important test-bed for this kind of question. Its spins are naturally associated with magnetic domains, and can be coupled by different physically motivated interactions. It turns out that random fields with cluster updates give rise to Barkhausen noise [1], local spin inversion symmetry is needed for memory effects [2], random couplings produce multicycles at low temperatures [3], while long-range and anisotropic interactions give domain patterns very similar to those in some real thin films [4].

The present work reports one more result of this kind: allow local diffusion of antiferromagnetic (AF) couplings, and the saturation part of the hysteresis curve will change, from the usual horizontal line to a figure-eight form. Such anomalies are sometimes observed in experiments on thin films and tapes, when the coercive fields are of the order of 100 Oe. We are aware of only one paper, however, where the authors have specifically commented upon them [5]. It is known from a diffraction experiment, albeit with domain structure carefully controlled by micromachining, that spatial evolution of AF couplings can occur under driving by a field [6]. We suggest here that a physically similar, but random, mechanism may be responsible for figure-eight shapes in saturation curves, in the usual situation, where sample domain structure is left to chance.

## II. THE MODEL

We use the same model as before [7]. Take the two-dimensional short-range bond-disordered Ising model, or  $\pm J$ -Edwards-Anderson (EA) model [8]

$$H = - \sum_{\langle i,j \rangle} J_{ij} S_i S_j - B \sum_i S_i \quad (1)$$

where  $J_{ij} = \pm J$  and  $S_i = \pm 1$ . The model is subject to Glauber [9] dynamics: spin is flipped at random, and the move is accepted if the criterion

$$\frac{1}{1 + \exp(\Delta/T)} > c$$

is satisfied, where  $\Delta$  is the energy balance of the trial move,  $T$  the temperature, and  $c$  a uniformly distributed random number,  $0 < c < 1$ . Between each two spin trials there is a bond trial: a positive and negative bond impinging on

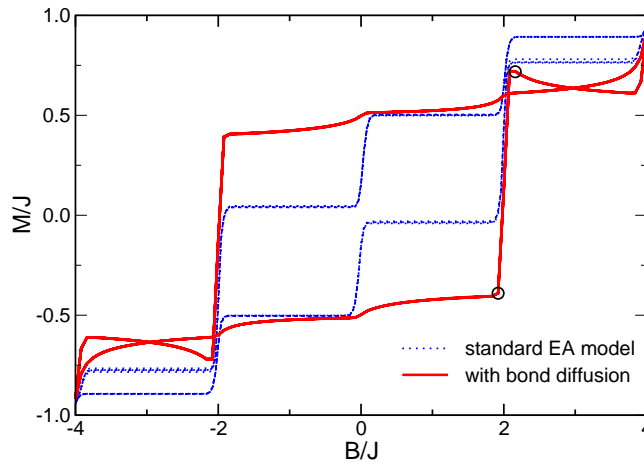


FIG. 1: Hysteresis in the model (1), with (full curve) and without (dotted curve) bond updates. Time spent at each field is ten updates per site. The initial parts of the loops have been erased for clarity. Note that the half-width of the main loop is the same as the range of each figure eight, namely  $2J$ . Open circles: see Fig. 4.

the same site, and chosen at random, are allowed to exchange places, subject to the same criterion as the spin trials. The concentration  $p_{AF}$  of antiferromagnetic (AF) bonds is taken to be 50%, unless otherwise noted.

This dynamics causes a significant annealing of the sample, and after a transient of  $\sim 100$  updates per site it enters a long-lived state characterized by glass-like dynamics, with a second, much longer relaxation time [7]. The ‘glassiness’ of the metastable state is not topological: the underlying bond distribution, viewed at any instant in time, has low frustration, so much so that it can be mapped onto a disordered ferromagnet [10], with a finite transition temperature [11]. However, when the bonds move, the spins are prevented from settling down into any given ordered arrangement. In this sense the situation is more reminiscent of the ‘geometric’ frustration of vitreous liquids, than of spin glasses: configurations are locally relaxed, but the spin correlation decays over time even at low temperature. As long as the number of F and AF bonds is kept equal, the equilibrium zero-field magnetization is zero.

The equivalent disordered ferromagnet is obtained by local gauge transformations which change the sign of bonds whenever the plaquette is not frustrated. The disorder in the ferromagnet comes from the residual AF bonds, related to the frustrated plaquettes, which are relatively few, so a net magnetization can appear, revealing the formerly hidden order. (This is different from a dilute ferromagnet, where some bonds have been assigned  $J = 0$ .) The degree of frustration, hence the order associated with the hidden ferromagnet, can change as a function of external field, because of bond diffusion. This is specific to the present model. In the usual situation without bond updates, the frustration is fixed for a given sample, and when  $p_{AF} = 50\%$ , the equivalent ferromagnet has no phase transition at finite temperature, and neither has the spin glass.

### III. MAIN RESULT

The model is subjected to a periodic external field, starting with  $B = 0$  and increasing to  $B = 4J$ , then reducing the field to  $B = -4J$ , and finally closing the curve. At each point in the field, we take 10 updates per site (meaning 10 spin and 10 bond updates in alternation). The dependence on this number (sweep rate) will be discussed in the next section. Two field steps were used,  $\Delta B = 0.04J$  and  $\Delta B = 0.08J$ , with no discernible difference in the results. We note that for our two-dimensional square lattice,  $B = 4J$  is the limit at which saturation is enforced, at a magnetization determined only by the temperature. The outcome is shown in Fig. 1, compared to the case without bond updates. The latter has been studied before [12] for the 3D case. Its hysteresis curve consists of a set of box-like regions, with constant magnetization alternating with large avalanches. This is easily understood, because the system is essentially in the clean limit. Namely, an individual Ising spin has only a finite, discrete set of energy values available. As soon as the external field passes through one of these values, all the respective spins are destabilized at the same time, and there is nothing to stop the ensuing avalanche. This result corresponds to low temperature ( $T = 0.1J$ ), on which we concentrate in the greater part of the article. Note that with a discrete set of bond strengths, the system is gapped, so the temperature  $T = 0.1J$  gives nearly the same results as  $T = 0.01J$ , except that the figure eight is slightly shifted, an insignificant effect to the purposes of this article.

Bond updates are now introduced, alternating equally with spin updates. It is no longer necessary to average

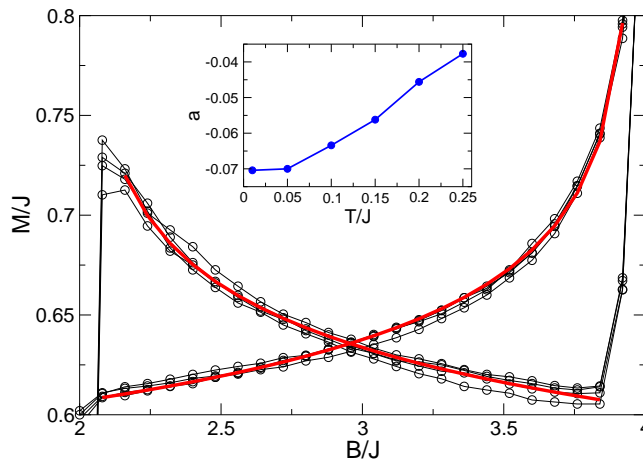


FIG. 2: Magnified figure-eight anomaly of Fig. 1, fitted (thick curves) to  $B^a$  with  $a = -0.07$ . The value of  $a$  is the same in the ascending and descending parts. Circles are raw data over four cycles. Inset: dependence of the exponent on the temperature.

over samples, because bond movement makes the whole sample space available to a single walker, or in technical terms, it induces self-averaging. This is so efficient that Fig. 1 simply gives the raw data for five cycles, showing how the corresponding points fall on the same curve, meaning the error bars are smaller than the line thickness. The simulations were mainly on  $100 \times 100$  lattices, with spot-checks to make sure that  $50 \times 50$  and  $200 \times 200$  gave the same results. The curves were also independent of the random initial conditions, given that field cycling began after the above-mentioned fast transient (50–100 MCS per site) died out.

Bond movement introduces two new features in Fig. 1. First, the two inner boxes (around the origin) open up into a single large one, with avalanches at  $B = \pm 2J$ . This is similar to what happens when a random static site field is added to the model without bond movement, or for a Gaussian distribution of bond strengths. It can be explained by the disappearance of spins intrinsically in an indifferent state, surrounded by the same number of positive and negative bonds, which are responsible for the avalanches at zero field. However, the reason for the disappearance is somewhat different in the two cases. Introducing site disorder of some characteristic magnitude  $K$  will make the formerly indifferent spins unstable at some new field values  $B \approx \pm K \neq 0$ , leaving few to participate in the avalanche at  $B = 0$ . In the present model, on the other hand, bond movement induces significant relaxation of the system, meaning most spins are in a locally minimal configuration, so again the number of indifferent ones is low.

The second new feature is somewhat unexpected. The former small box at  $2J < B < 4J$  is now a distinct figure-eight loop. Both the forward (increasing  $B$ ) and backward (decreasing  $B$ ) parts of the magnetization curve have the form of relaxation curves. They are given by power laws in  $B$  with small exponents, as shown in Fig. 2. By contrast, the temporal autocorrelation of the magnetization is a stretched exponential, as in other similar models. Hence the  $M(B)$  curves cannot be interpreted as a simple temporal evolution, trivially due to the fact that  $B$  changes before the system has had time to equilibrate. The bond updates introduce a new relaxation mechanism, with a scale comparable to the scale of the main cycle. The exponent of  $B$  becomes (absolutely) smaller as the temperature increases, which reflects the figure-eight becoming thinner and flatter. The temperature dependence of the exponent is given in the inset to the figure.

The main avalanche in this model is microscopically different than in models with quenched disorder, because in the presence of bond updates, the frustration of the lattice can vary as a function of the field. This is shown in Figure 3. In the region of the main loop, the equivalent disordered ferromagnet has a finite transition temperature. The concentration of frustrated plaquettes rises sharply with the main avalanche, and passes through the critical value, above which the ferromagnet has  $T_c = 0$ . In this way the spin avalanche is connected with a ground-state transition in the bond lattice. For  $B < 2J$ , the instantaneous bond configuration can support an ordered spin state at finite temperature; above this value, it cannot.

In Fig. 4, sample configurations are shown immediately before and after the main avalanche. In the ordered state, there are islands of spins with the same orientation (dot: up, circle: down), connected by ferromagnetic bonds. In the disordered state, the islands of down-spins (circles) have broken up, and each is preferentially connected with up-spins by ‘crosses’ of AF bonds.

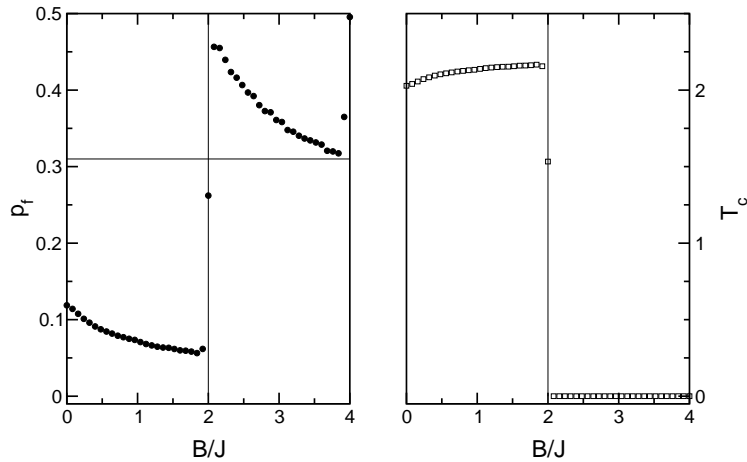


FIG. 3: Left: concentration of frustrated plaquettes as a function of the field, for the full curve in Fig. 1. Horizontal line: critical value  $p_c = 0.31$  at which  $T_c = 0$  for the equivalent disordered ferromagnet. Right: transition temperature of the latter, obtained from the values in the left panel according to Ref. [11].

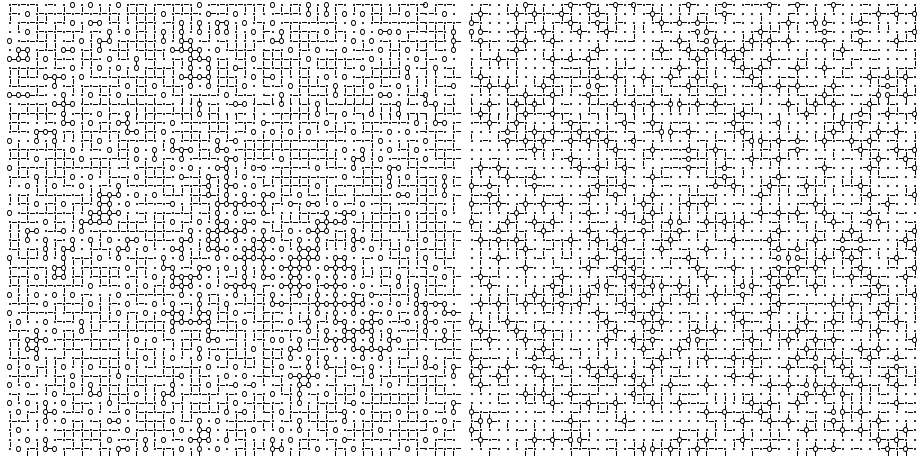


FIG. 4: Configurations before and after the main avalanche. Left: ordered state, lower open circle in Fig. 1. Only ferromagnetic bonds are shown. Right: disordered state, upper open circle in Fig. 1. Only AF bonds are shown. Circles: down-spins. Dots: up-spins.

#### IV. PHENOMENOLOGY OF THE MODEL

In this section, we show how the basic curve in Fig. 1 changes with various aspects of the model dynamics. There are three to which it should be at least moderately robust: temperature, ratio of spin to bond updates, and sweep rate.

In Figure 5, we observe that the figure-eight evolves with temperature on the scale of  $J$ . At  $T = 0.5J$ , the first maximum of the figure eight has dropped below the reverse curve, so there is now an open narrow loop at  $B > 2J$ , which is still wider at the middle than at either end. The narrowing of the main part  $-2J < B < 2J$  is significantly milder than in the case without bond updates [12], so that, overall, their introduction makes the hysteresis less sensitive to temperature increase.

In Figure 6, we show that the figure-eight feature is not a transient effect due to too fast cycling. It visibly persists to up to 500 updates/site at each field, although it becomes thinner. We know that in the model's two-time dynamics, the transition between the fast (transient) and slow (metastable equilibrium) component occurs at 50–100 updates per site, so the feature survives into the intrinsic ‘glassy’ regime. Observed figure-eight anomalies are indeed thinner (relative to the main loop) than suggested by Fig. 1. This agrees with the idea that experimentally, magnetizations at each point of the loop are measured after any fast transients have died out. We find, nevertheless, that the power-law relaxation of  $M$  with  $B$  is found in all three curves in Fig. 6, so it is not wrong to use fast cycling for

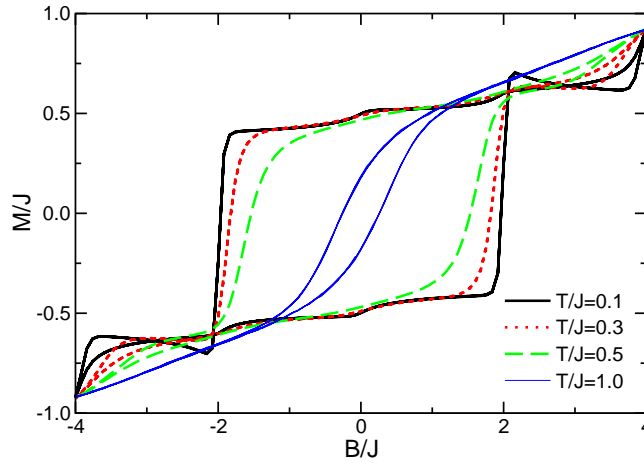


FIG. 5: Temperature dependence of the hysteresis. Thick full line:  $T = 0.1J$  (Fig. 1). Dotted line:  $T = 0.3J$ . Broken line:  $T = 0.5J$ . Thin full line:  $T = J$ .

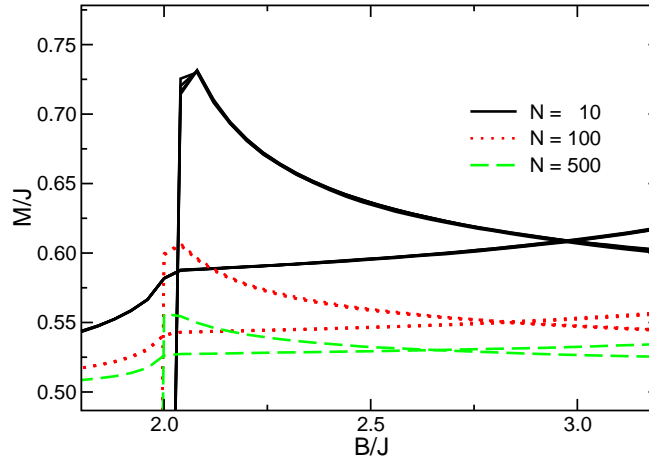


FIG. 6: Dependence of the figure-eight feature on the time spent at each field. Full line: 10 updates/site (Fig. 1). Dotted line: 100 updates. Broken line: 500 updates. The field step is  $\Delta B = 0.04J$  in all three curves.

model investigations. Only the numerical value of the relaxation exponent changes, decreasing with slower cycling. Increasing the number of updates at each field also gets rid of the steps at  $B = 0$  in Fig. 1, without changing the shape and size of the main loop.

In Figure 7, we show perhaps the most unexpected outcome of the phenomenological investigations. We vary the relative frequency of spin and bond updates, guided by the idea that they are not equally common in real materials. Based on past modelling experience, one would assume that bond updates should be rarer, so it matters that the figure-eight is not too sensitive to their rate. Indeed it is not, but it also turns out that the system responds much the same whether it is the rate of spin or bond updates that is decreased. Hysteresis curves in which they differ by a factor of ten either way fall practically on top of each other. Bond updates are therefore efficient in mutually equilibrating the spin and bond subsystems. They are out of equilibrium with respect to the asymptotic state, but not with respect to each other. Figure 7 also shows a dependence on the total number of updates at each field value, *i.e.* the sweep rate, like in Fig. 6. The curves with opposite ratios of spin to bond updates are similar only if the sum of the updates is the same. The thin full line has the same ratio of the two as the dash-dotted line, but shows the effect of faster cycling, with a more pronounced figure eight, and noisier magnetization. (Note that the  $N = 10$  curve in Fig. 6 has the same number of updates as the thick full line in Fig. 7.)

In fact, it turns out that the  $\pm J$ -Edwards-Anderson model is extremely sensitive to the introduction of bond updates. Take the  $T/J = 0.3$  curve in Fig. 5, obtained with a 1:1 ratio of bond to spin updates. Going down to 1:200 barely changes it: it becomes something like the  $T/J = 0.5$  curve in the same figure. But turning off bond updates entirely collapses the main loop to the two boxes shown in Fig. 1.

Finally, we find that the figure-eight is quite sensitive to noise in the bond couplings. A Gaussian spread with

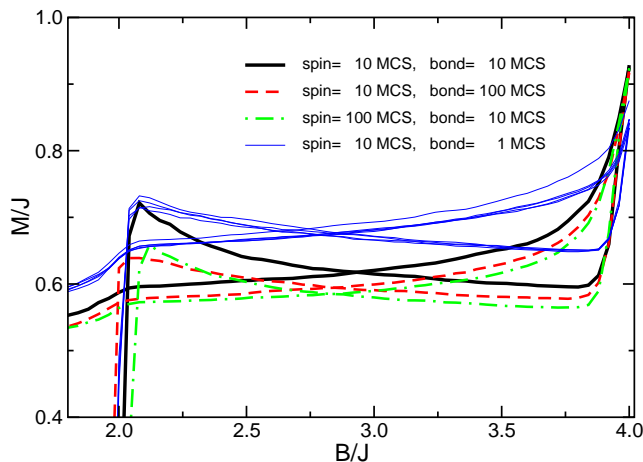


FIG. 7: Dependence of the figure-eight feature on the ratio of spin to bond updates, at  $T = 0.05J$ . Raw data for five cycles are shown for each curve. See the text for details.

$\sigma = 0.05J$  centered at  $\pm J$  is sufficient to flatten it almost completely. Thus while it can survive some noise in the bond distribution — *i.e.* is not a singular effect — the figure-eight anomaly should at present be regarded as specific to the  $\pm J$  model.

## V. EXPERIMENTAL EVIDENCE

Experimental observations of the figure-eight anomaly are not very rare, but it is rare that anyone comments on them; in fact we found only one paper in which this was explicitly mentioned as an unexplained phenomenon [5]. This may partly be because such forms can be dismissed as artefacts, due to the integration of a noisy differential signal  $dM/dH$  in the saturation region, where the derivative is small. Another possible reason is that they are sometimes observed [13] along with a number of other ‘misfeatures,’ such as a marked absence of inversion symmetry relative to the origin in the  $(B, M)$  plane, so it is not clear that they should be singled out for attention.

In Ref. [13], annealed amorphous samples of  $\text{Co}_{66}\text{Fe}_4\text{B}_{15}\text{Si}_{15}$  with a recrystallized surface were studied by the magneto-optical effect. The surface was chemically etched to expose the amorphous interior of annealed samples, and the changes in the hysteresis curves recorded. After etching for ten minutes, the magnetic response became softer and a thin but distinct figure-eight appeared in the saturation region. Since the laser is a local probe, it was also possible to obtain hysteresis curves at different physical positions on the as-quenched sample surface. Some of these also show a figure eight, which the authors do not comment. The width of the measured ‘boxy’ main loop (large avalanche!) in the field was of the same order as the range of the figure eight, just as found in the model calculations here (see Fig. 1).

In Ref. [6], a thin-film grating was subject to a periodic field and the magnetic order observed by X-ray scattering. A perfectly reproducible AF ordering was observed at both values of the coercive field, *i.e.* as the sample passed through zero magnetization. This does not mean that the positions of the effective AF (dipolar) couplings among the domains has been changing, in fact quite the opposite, it is proof that it is fixed. The interesting observation from our point of view occurred during sample preparation. Direct observation of magnetic domains in ‘fresh’ samples showed they did not follow the lines of the grating, but were in fact quite random, so that the grating geometry could barely be discerned. A careful demagnetization process, with a slowly vanishing field, was necessary to arrange the domains along the grating lines. During this process, the effective couplings were evidently rearranged in space. Once they ‘fell into line,’ they did not evolve any further. We suggest a similar evolution is happening in ordinary ‘fresh’ samples, without control of domain positions. First there is some rearrangement of domains under field cycling, amounting to a spatial evolution (diffusion) of AF bonds. As the sample ages, the domain positions should become fixed, pinned perhaps by impurities, and the figure-eight anomaly should disappear. This scenario is corroborated in Ref. [13], whose authors observed a hardening of the magnetic response and disappearance of the anomaly after eight hours of annealing, which recrystallized the surface. When the sample was etched as described above, the anomaly reappeared.

## VI. DISCUSSION

Hysteretic effects are to be expected whenever the approach to thermal equilibrium is somehow hindered. One widely studied way in which this can happen is when the equilibrium state is itself disordered, and the system takes a long time to find this state among the many suboptimal, similarly disordered ones. This is the case of spin glasses, especially in two dimensions where the spin-glass transition temperature is zero. A different way to hinder equilibration is provided by kinetic glasses, where the underlying equilibrium state is ordered, but is never reached because of kinetic obstruction.

The use of the disordered Ising model with fixed bond distribution to study hysteresis assumes that the metastability involved in magnetic hysteresis may have something in common with the metastability of spin glasses. This is tacitly assumed in all such investigations of hysteresis with fixed bond distributions. The present work investigates the alternative possibility, that the delayed thermalization in magnetic hysteresis may be more like the metastability of kinetic glasses. The figure-eight anomaly was identified as a distinct and sensitive signal of this latter scenario. Experimental observations [6] allow that a real-space redistribution of effective AF interactions between magnetic domains can be driven by an external field, with response times within the experimental window. One would intuitively expect this rearrangement capability to decrease as the sample ages. Indeed this seems to be the case in the experiment mentioned above [13].

The above observations open some interesting theoretical issues, as well. One is a possible connection between the hidden order-disorder transition in the bond background at the main avalanche, and the appearance of the figure-eight anomaly in the state disordered by the field. A related issue is to understand the origin of the power-law relaxation of the magnetization as a function of the field. Another is the dependence of the anomaly on the distribution of bond couplings — we know, for example, that there is no anomaly for a unimodular Gaussian distribution. These questions are currently under investigation.

To conclude, we have given a simple interpretation of the figure-eight anomaly, sometimes observed in magnetic thin films and tapes in the saturation region, when the coercive fields involved are relatively weak, of the order of 100 Oe. We believe it is related to a specific transient process, which may be represented as a spatial rearrangement of AF (dipolar) couplings in the sample, driven by the field.

## VII. ACKNOWLEDGEMENTS

Conversations with K. Uzelac and I. Campbell are gratefully acknowledged. This work was supported by the Croatian Government under Project 0119256.

- 
- [1] J. P. Sethna, K. A. Dahmen, S. Kartha, J. A. Krumhans, B. W. Roberts, and J. D. Shore, *Phys. Rev. Lett.* **70**, 3347 (1993).
  - [2] H. G. Katzgraber, F. Pázmándi, C. R. Pike, K. Liu, R. T. Scalettar, K. L. Verosub, and G. T. Zimányi, *Phys. Rev. Lett.* **89**, 257202 (2002).
  - [3] J. M. Deutsch and O. Narayan, *Phys. Rev. Lett.* **91**, 200601 (2003).
  - [4] J. R. Iglesias, S. Gonçalves, O. A. Nagel, and M. Kiwi, *Phys. Rev. B* **65**, 064447/1 (2002).
  - [5] C. A. dos Santos and B. Rodmacq, *J. Magn. Magn. Mater.* **147**, L250 (1995).
  - [6] K. Chesnel, M. Belakhovsky, S. Landis, J. C. Toussaint, S. P. Collins, G. van der Laan, E. Dudzik, and S. S. Dhesi, *Phys. Rev. B* **66**, 024435/1 (2002).
  - [7] P. Lazić and D. K. Sunko, *Eur. Phys. J. B* **21**, 595 (2001).
  - [8] S. F. Edwards and P. W. Anderson, *J. Phys. F* **5**, 965 (1975).
  - [9] R. J. Glauber, *J. Math. Phys.* **4**, 294 (1963).
  - [10] A. K. Hartmann, *Phys. Rev. B* **67**, 214404 (2003).
  - [11] F. Merz and J. T. Chalker, *Phys. Rev. B* **65**, 054425 (2002).
  - [12] E. E. Vogel, J. Cartes, D. Altbir, and P. Vargas, *J. Magn. Magn. Mater.* **226-230**, 1248 (2001).
  - [13] C. G. Kim, Y. W. Rheem, C. O. Kim, E. E. Shalyguina, and E. A. Ganshina, *J. Magn. Magn. Mater.* **262**, 412 (2003).